


Half-quantum vortex pair in the polar-distorted B phase of superfluid ^3He in aerogels

Masaki Tange and Ryusuke Ikeda

Department of Physics, Graduate School of Science, Kyoto University, Kyoto 606-8502, Japan
 (Received 5 December 2019; revised manuscript received 12 February 2020; accepted 21 February 2020; published 12 March 2020)

Motivated by the recent observation and argument on a large half-quantum vortex (HQV) pair connected by a Kibble-Lazarides-Shafi wall in superfluid ^3He in nematic aerogels, we numerically study to what extent a huge HQV pair can intrinsically occur in the polar-distorted B (PdB) phase of superfluid ^3He . First, the “impurity”-scattering model used in a previous study is extended to a form interpolating the weakly and strongly anisotropic cases, and it is found that, within the Ginzburg-Landau (GL) approach, Anderson’s theorem is satisfied in the strongly anisotropic case. By taking account of the Fermi-liquid (FL) corrected gradient terms and solving numerically the resulting GL free energy, the anisotropy dependence of the vortex structure minimizing the free energy is examined within the weak-coupling approximation. It is found that, close to the transition between the polar and PdB phases, an interplay of the strong anisotropy and the FL correction makes possible the emergence of a large HQV pair in the PdB phase, and that, nevertheless, such a large pair easily shrinks upon deeply entering the PdB phase, indicating that a pinning effect due to the aerogel structure is necessary in order to keep a large pair size there. The obtained result indicates the validity of the London limit for describing the vortex structure, and a consistency with the picture based on the NMR measurement is discussed.

DOI: [10.1103/PhysRevB.101.094512](https://doi.org/10.1103/PhysRevB.101.094512)**I. INTRODUCTION**

The recent observation of half-quantum vortices (HQVs) [1] in the novel polar phase of superfluid ^3He has created a new avenue for studying possible vortices in a fermionic superfluid phase. The emergence of the three-dimensional (3D) polar phase in anisotropic aerogels has been proposed through a model calculation [2] assuming a weak anisotropy, and it has been experimentally verified in nematic aerogels [3]. A nematic aerogel has its strands aligned to one direction and can be regarded, broadly speaking, as a collection of linelike obstacles. The HQV was originally expected to be realized in the thin-film configuration of the chiral superfluid A phase with its orbital angular momentum locked perpendicular to the film plane [4,5]. However, the chiral A phase is realized with the help of the strong-coupling correction, which is effective at higher pressures, while it has been clarified [6] that the HQV tends to be destabilized by the strong-coupling correction. Fortunately, the polar phase realized in the nematic aerogel has a wider temperature range of its stability at relatively lower pressures, and hence superfluid ^3He in the nematic aerogels becomes the best playground for studying this novel topological object.

Recently, an experimental investigation of the vortices in nematic aerogels was extended to lower temperatures [7], and HQVs have also been detected in the A and B phases realized at lower temperatures in the nematic aerogels. Since such A and B phases in nematic aerogels are distorted by an anisotropy in the scattering events due to the aerogel structure, the resulting A and B phases will be referred to hereafter as the polar-distorted A (PdA) and polar-distorted B (PdB) phases following Ref. [7]. It has been suggested that the detected HQV-pairs do not change their positions upon both cooling

from and warming to the polar phase, and hence that, since in their rotated experiments the rotation axis is parallel to the direction in which the strands are aligned, the realization of such surprising observations is largely supported by a strong pinning effect due to the linelike aerogel structure [7]. However, just the method of analyzing the NMR data in the PdB phase on the basis of a hypothetical description of the vortex structure in the London limit has been presented in Ref. [7], and the validity of their London description has not been examined there. Once we take into account the fact that the core structure of the stable vortex, called the double-core vortex, in the bulk B phase at lower pressures is regarded [8,9] as a pair of HQVs, it is natural to imagine that the core structure of the double-core vortex has transformed to a HQV pair loosely connected by a nontopological Kibble-Lazarides-Shafi (KLS) wall defect [7,10] in the PdB phase. A couple of questions then arise: How does the vortex core structure, in which variations of the various components of the order parameter are usually remarkable [11,12] in the bulk B phase, change to a simple HQV-pair, for which the London description [5,7] is valid, in the PdB phase? Further, do the huge HQV pairs detected in the PdA and PdB phases disappear if the pinning effect of the aerogel structure becomes negligible?

In the present work, we start by reformulating the Ginzburg-Landau (GL) approach for describing superfluid ^3He in anisotropic aerogels by extending the weakly anisotropic model [2] of the impurity-scattering potential to the strongly anisotropic case appropriate for the situations in the nematic aerogels [1,3,13]. The uniaxial anisotropy will be introduced in this work via the size of the correlation length on the impurity potential. Using the GL free energy following from our microscopic analysis, stable vortex solutions are studied in both the polar and PdB phases in strongly

anisotropic cases. Throughout this work, we focus on the weak-coupling approximation, neglecting the strong-coupling correction to the bulk free-energy terms because a theory of the strong-coupling correction in the impure and strongly anisotropic case has not been formulated so far. For this reason, the PdA phase never appears in the present results, and we have only a direct continuous transition between the polar and PdB pairing states. Since superfluid ^3He in globally isotropic aerogels, which has essentially the same vortex solution as in the bulk liquid case, can be consistently studied within our model, we examine how the tightly bound HQV pair forming the vortex core in the bulk B phase is changed to a simple HQV pair connected by a KLS wall upon increasing the anisotropy. It is found that, as the anisotropy is increased, the description based on the London limit of the order-parameter profiles of one HQV-pair becomes better. Furthermore, as the anisotropy is increased, the separation between the two HQVs forming one pair is increased and becomes macroscopic, particularly close to the transition temperature T_{PB} between the polar and PdB phases. However, this size rapidly shrinks upon cooling from T_{PB} , reflecting the resulting increase upon cooling of the tension of the KLS wall, which is in the polar-distorted planar state [14]. This implies that, deep in the PdB phase, a HQV pair with a macroscopic size is not naturally stabilized, and hence that the survival of a huge HQV pair there justifies the picture [7] of a HQV pair stabilized by the pinning due to the linelike aerogel structure.

The present paper is organized as follows. In Sec. II, the vertex correction to the pairing process is explained in detail together with the model of the impurity scattering used in this work. In Sec. III, the resulting GL free energy affected by the impurity effects is explained. In Sec. IV, it is explained how a HQV pair in the PdB phase is stabilized within the description in the London limit. Our numerical results and detailed discussions about them are presented in Sec. V, and a summary and discussions are given in Sec. VI. Details on the impurity-induced vertex correction and its effects on the $O(|\Delta|^4)$ gradient terms are explained in two Appendixes.

II. MODEL OF IMPURITY SCATTERING

Our microscopic analysis for deriving the GL free energy is based on a BCS Hamiltonian with the nonmagnetic and random scattering potential term of the form

$$\mathcal{H}_{\text{imp}} = \int_{\mathbf{r}} \psi_{\sigma}^{\dagger}(\mathbf{r}) u(\mathbf{r}) \psi_{\sigma}(\mathbf{r}), \quad (1)$$

where $u(\mathbf{r})$ is a spin-independent random potential, and ψ_{σ} is a fermion operator with the spin index σ . Hereafter, we focus on the case in which the scattering process is nonmagnetic, since, in the experiments where the HQVs have been observed, the local surface of the aerogel is believed to be entirely coated by ^4He so that the spin-flip scattering between the ^3He atoms solidified on the surface and the quasiparticles of liquid ^3He is ineffective. Regarding the random averaging over $u(\mathbf{r})$, the Fourier transformation $u_{\mathbf{k}}$ of $u(\mathbf{r})$ is assumed to have zero mean and the mean-squared average,

$$\overline{|u_{\mathbf{k}}|^2} = \frac{1}{2\pi N(0)\tau} w(\mathbf{k}). \quad (2)$$

In the original work [2], a weak stretched anisotropy has been incorporated in $w(\mathbf{k})$ in the form

$$w(\mathbf{k}) = 1 + \delta_u \hat{k}_z^2, \quad (3)$$

where $\hat{k}_z = k_z/k_F$, and we have followed the notation in Ref. [2] where, when $\delta_u < 0$, a narrow range of the polar phase has been proposed to appear in an aerogel sample stretched along the z -direction. For this reason, the z -axis will be referred to hereafter as the polar axis, and, as an extension of this impurity-scattering model to the case in a strongly anisotropic aerogel, the following model on $w(\mathbf{k})$ will be used:

$$w(\mathbf{k}) = \frac{1 + (\sqrt{|\delta_u|} - 1)\Theta(|\delta_u| - 1)}{1 + |\delta_u|\hat{k}_z^2}, \quad (4)$$

where $\Theta(x)$ is the step function: $\Theta(x > 0) = 1$, and $\Theta(x < 0) = 0$. The factor $\sqrt{|\delta_u|}$ in Eq. (4) in $|\delta_u| \geq 1$ is necessary to obtain a physically reasonable limit of the quasiparticle relaxation rate in $|\delta_u| \rightarrow \infty$.

We note that the Fourier transformation of Eq. (4) is given by

$$W(\mathbf{r}) = 2\pi N(0)\tau \overline{u(\mathbf{r})u(0)} = \frac{k_F}{2} \delta^{(2)}(\mathbf{r}_{\perp}) \times e^{-|z|/L_z} [1 + \Theta(1 - |\delta_u|)(|\delta_u|^{-1/2} - 1)], \quad (5)$$

where $|\delta_u| = k_F^2 L_z^2$. Thus, the anisotropy parameter $|\delta_u|$ is a measure of the correlation length L_z defined along the polar axis of the impurity potential.

In the weakly anisotropic limit where $|\delta_u| \ll 1$, this expression reduces to Eq. (3), while in the opposite strongly anisotropic limit where $|\delta_u| \rightarrow +\infty$, i.e., $L_z \rightarrow +\infty$, Eq. (4) approaches the quantity

$$w_{\infty}(\mathbf{k}) = \pi k_F \delta(k_z), \quad (6)$$

or equivalently, Eq. (5) becomes z -independent. Equation (6) implies that, in the limit of strong anisotropy, the scattering event is specular along the polar axis. This corresponds to the model proposed by Fomin [15] regarding the nematic aerogels as a collection of columnar defects.

To derive a GL free energy incorporating the scattering processes due to the aerogel structure with any strength of the anisotropy, we need a renormalized pairing vertex Λ_j replacing the bare pairing vertex $\hat{p}_j = p_j/k_F$, which depends not only on the relative momentum \mathbf{p} but also on the center-of-mass momentum \mathbf{Q} and the fermion Matsubara frequency ε . The Bethe-Salpeter equation sketched in Fig. 1,

$$\Lambda_j(\hat{\mathbf{p}}; \mathbf{Q}) = \hat{p}_j + \frac{1}{2\pi N(0)\tau} \int_{\mathbf{p}'} \Lambda_j(\hat{\mathbf{p}}'; \mathbf{Q}) \times \mathcal{G}_{\varepsilon}(\mathbf{p}' + \mathbf{Q}/2) \mathcal{G}_{-\varepsilon}(-\mathbf{p}' + \mathbf{Q}/2) w(\mathbf{p} - \mathbf{p}'), \quad (7)$$

for Λ_j can be solved in a closed form by assuming Λ_j to take the expression

$$\Lambda_i(\hat{\mathbf{p}}; \mathbf{Q}) = \hat{p}_j \left\{ \delta_{ij}^{(z)} + \hat{z}_j [\hat{z}_i C(\mathbf{Q}) + v Q_i v Q_z C_{1z}] \right\} - i s_{\varepsilon} v Q_j \left\{ \delta_{ij}^{(z)} B(\hat{p}_z) + \hat{z}_i \hat{z}_j [B(\hat{p}_z) + D(\hat{p}_z)] \right\}, \quad (8)$$

where

$$\mathcal{G}_{\varepsilon}(\mathbf{p}) = (i\varepsilon_{\mathbf{p}} - \xi_{\mathbf{p}})^{-1} \quad (9)$$

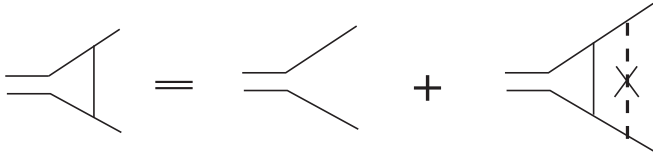


FIG. 1. Diagram expressing the Bethe-Salpeter equation that the vertex function Λ (triangle) obeys. The straight solid lines denote normal Green's functions, and the impurity average of the squared random potential is expressed by a dashed line with a cross.

is the Matsubara Green's function with the self-energy term including the impurity scattering, $\xi_{\mathbf{p}}$ is the quasiparticle energy, and $\tilde{\xi}_{\mathbf{p}}$ will be given by Eq. (A1) in Appendix A. Furthermore, $\delta_{ij}^{(z)} = \delta_{ij} - \hat{z}_i \hat{z}_j$, $s_\varepsilon = \varepsilon/|\varepsilon|$, $v\hat{p}_j$ is the Fermi velocity, and

$$\begin{aligned} C(\mathbf{Q}) &= C_0(\varepsilon) + C_{21}(\varepsilon)v^2Q^2 + C_{2z}(\varepsilon)v^2Q_z^2, \\ B(\hat{p}_z) &= B_0(\varepsilon) + \Delta B(\varepsilon)\hat{p}_z^2, \\ D(\hat{p}_z) &= D_0(\varepsilon) + \Delta D(\varepsilon)\hat{p}_z^2. \end{aligned} \quad (10)$$

The general form of Λ_j is involved and will be presented in Appendix A. Here, just its limiting behaviors will be explained. First, in the isotropic limit where $\delta_u \rightarrow 0$, $C_0 \rightarrow 1$, and other coefficients except B_0 vanish. Then, Λ_i reduces to

$$\Lambda_i^{(0)} = \delta_{ij} \left(\hat{p}_j - is_\varepsilon v Q_j \frac{1}{12\tau|\varepsilon\tilde{\varepsilon}_0|} \right), \quad (11)$$

where $|\tilde{\varepsilon}_0| = |\varepsilon| + 1/(2\tau)$. As stressed elsewhere [16], the divergent behavior proportional to $|\varepsilon|^{-1}$ in the second term of Eq. (11) is a consequence of cancellation between the quasiparticle relaxation rate and the impurity-ladder vertex correction, and it can be seen as being of the same origin as the impurity scattering-independent transition temperature in the s -wave superconductor [17].

In the opposite limit where $|\delta_u| \rightarrow +\infty$, i.e., the limit of strong anisotropy, the coefficients in Λ_j approach the following expressions:

$$\begin{aligned} B_0 &\simeq -\Delta B = -D_0 = \frac{\pi}{16|\varepsilon\tilde{\varepsilon}_\infty|\tau}, \\ \Delta D &\simeq -D_0 + \frac{\pi}{8\varepsilon^2\tau}, \end{aligned}$$

$$\begin{aligned} C_0 &\simeq \frac{|\tilde{\varepsilon}_\infty|}{|\varepsilon|}, \\ C_{21} &\simeq -\frac{\pi}{32\varepsilon^2|\tilde{\varepsilon}_\infty|\tau}, \\ C_{1z} &\simeq -\frac{\pi}{16\tilde{\varepsilon}_\infty^2|\varepsilon|\tau} \left(1 + \frac{\pi}{8|\varepsilon|\tau} \right), \end{aligned} \quad (12)$$

and $C_{2z} = -C_{21} - C_{1z}$, where $|\tilde{\varepsilon}_\infty| = |\varepsilon| + \pi/(4\tau)$. Then, Λ_j reduces to

$$\begin{aligned} \Lambda_i^{(\infty)} &= \delta_{ij}^{(z)} \left(\hat{p}_j - is_\varepsilon \frac{\pi}{16|\varepsilon\tilde{\varepsilon}_\infty|\tau} v Q_j \hat{p}_\perp^2 \right) + \hat{z}_i \hat{z}_j \frac{|\tilde{\varepsilon}_\infty|}{|\varepsilon|} \\ &\times \left[\hat{p}_j \left(1 - \frac{\pi}{32\tilde{\varepsilon}_\infty^2|\varepsilon|\tau} v^2 Q_\perp^2 \right) - is_\varepsilon \hat{p}_z^2 \frac{\pi}{8|\varepsilon\tilde{\varepsilon}_\infty|\tau} v Q_j \right] \\ &- \delta_{ij}^{(z)} \mathbf{Q}_j \frac{\pi}{16\tilde{\varepsilon}_\infty^2|\varepsilon|\tau} \left(1 + \frac{\pi}{8|\varepsilon|\tau} \right) v^2 \hat{p}_z Q_z, \end{aligned} \quad (13)$$

where $\hat{p}_\perp^2 = 1 - \hat{p}_z^2$. We note that the second term of $|\tilde{\varepsilon}_\infty|$ corresponds to the imaginary part of the self-energy of the normal Green's function. The Q_\perp^2 term in Eq. (13) suggests the presence of a diffusion pole $(2|\varepsilon| + v^2\tau Q^2/\pi)^{-1}$. Each coefficient in Eq. (8) is reflected in each term of the GL free energy, which will be given in the next section and Appendix A.

III. RESULTING GL FREE ENERGY

We will use an appropriate GL free energy to numerically study the vortex solutions stable in anisotropic aerogels. For our purpose of studying the vortex excitation with the lowest energy, the terms arising from spatial variations of the superfluid transition temperature T_c and acting as a pinning potential of a vortex will be neglected in the free energy written in terms of the order parameter field $A_{\mu i}$. Furthermore, any term accompanied by the repulsive channel of the quasiparticle interaction will not be considered in this section. Then, the GL free energy $F_{\text{GL}} = F_2 + F_4$ in the presence of the impurity-scattering effect, as usual, consists of the quadratic term

$$\begin{aligned} F_2/\Omega &= \sum_{\mathbf{Q}} \left\{ \frac{N(0)}{3} \left[\ln \left(\frac{T}{T_{c0}} \right) + T \sum_{\varepsilon} \frac{\pi}{|\varepsilon|} \right] \delta_{i,j} \right. \\ &- T \sum_{\varepsilon} \int_{\mathbf{p}} \hat{p}_i \Lambda_j(\hat{\mathbf{p}}, \mathbf{Q}) \mathcal{G}_{\varepsilon}(\mathbf{p} + \mathbf{Q}/2) \mathcal{G}_{-\varepsilon}(-\mathbf{p} + \mathbf{Q}/2) \left. \right\} \\ &\times A_{\mu i}^*(\mathbf{Q}) A_{\mu j}(\mathbf{Q}), \end{aligned} \quad (14)$$

and the quartic term

$$\begin{aligned} F_4/\Omega &= \frac{1}{2} [A_{\mu i}^* A_{\mu j} A_{\nu k}^* A_{\nu l} - A_{\mu i}^* A_{\nu j} A_{\mu k}^* A_{\nu l} + A_{\mu i}^* A_{\nu j} A_{\nu k}^* A_{\mu l}] \\ &\times T \sum_{\varepsilon} \int_{\mathbf{p}_1} \int_{\mathbf{p}_2} \int_{\mathbf{p}_3} \int_{\mathbf{p}_4} \Lambda_i(\hat{\mathbf{p}}_1; 0) \Lambda_j(\hat{\mathbf{p}}_2; 0) \Lambda_k(\hat{\mathbf{p}}_3; 0) \Lambda_l(\hat{\mathbf{p}}_4; 0) \mathcal{G}_{\varepsilon}(\mathbf{p}_1) \mathcal{G}_{-\varepsilon}(-\mathbf{p}_1) \mathcal{G}_{\varepsilon}(\mathbf{p}_3) \mathcal{G}_{-\varepsilon}(-\mathbf{p}_3) \\ &\times (\delta_{\mathbf{p}_1, \mathbf{p}_2} \delta_{\mathbf{p}_1, \mathbf{p}_3} \delta_{\mathbf{p}_1, \mathbf{p}_4} + \delta_{\mathbf{p}_1, \mathbf{p}_4} \delta_{\mathbf{p}_2, \mathbf{p}_3} \mathcal{G}_{\varepsilon}(\mathbf{p}_1) \mathcal{G}_{\varepsilon}(\mathbf{p}_2) |\overline{u_{\mathbf{p}_1 - \mathbf{p}_2}}|^2 + \delta_{\mathbf{p}_1, \mathbf{p}_2} \delta_{\mathbf{p}_3, \mathbf{p}_4} \mathcal{G}_{\varepsilon}(\mathbf{p}_1) \mathcal{G}_{\varepsilon}(\mathbf{p}_3) |\overline{u_{\mathbf{p}_1 - \mathbf{p}_3}}|^2), \end{aligned} \quad (15)$$

where $T_{c0}(P)$ is the normal to superfluid transition temperature of the bulk liquid at each pressure P , Ω is the volume, and, for simplicity, F_4 was written here by assuming the order parameter to be spatially uniform. Up to the lowest order in

the spatial gradient, one can separate $F_2 + F_4$ into the bulk energy contribution $F_{\text{bulk}} = \int_{\mathbf{r}} f_{\text{bulk}}$, where

$$\begin{aligned} f_{\text{bulk}} = & [\alpha + (\alpha_z - \alpha)\delta_{iz}]A_{\mu i}A_{\mu i}^* + \beta_1^{(0)}|A_{\mu i}A_{\mu i}|^2 \\ & + \beta_2^{(0)}(A_{\mu i}A_{\mu i}^*)^2 + \beta_3^{(0)}A_{\mu i}^*A_{\mu i}^*A_{\mu j}A_{\mu j} \\ & + \beta_4^{(0)}A_{\mu i}^*A_{\mu i}^*A_{\mu j}^*A_{\mu j} + \beta_5^{(0)}A_{\mu i}^*A_{\mu i}^*A_{\mu j}^*A_{\mu j}^* + \beta_z|A_{\mu z}A_{\mu z}^*|^2 \\ & + [\beta_1^{(1)}A_{\mu i}A_{\mu i}A_{\mu z}^*A_{\mu z}^* + \beta_2^{(1)}A_{\mu i}A_{\mu i}^*A_{\mu z}A_{\mu z}^* \\ & + \beta_3^{(1)}A_{\mu i}^*A_{\mu i}^*A_{\mu z}A_{\mu z} + \beta_4^{(1)}A_{\mu i}^*A_{\mu i}^*A_{\mu z}^*A_{\mu z} \\ & + \beta_5^{(1)}A_{\mu i}^*A_{\mu i}^*A_{\mu z}A_{\mu z}^* + \text{c.c.}], \end{aligned} \quad (16)$$

and the gradient terms. In the case of weak anisotropy where $|\delta_u| \ll 1$, the $\beta_n^{(1)}$ ($n = 1, \dots, 5$) terms appear in $O(|\delta_u|)$, while the β_z term first appears in $O(\delta_u^2)$.

Among the gradient terms, the free-energy density corresponding to the contributions from F_2 consists of the following seven terms:

$$\begin{aligned} f_{\text{grad}} = & 2K_1\partial_i A_{\mu i}\partial_j A_{\mu j}^* + K_2\partial_i A_{\mu j}\partial_i A_{\mu j}^* + K_3\partial_z A_{\mu i}\partial_z A_{\mu i}^* \\ & + K_4\partial_i A_{\mu z}\partial_i A_{\mu z}^* + K_5(\partial_i A_{\mu i}\partial_z A_{\mu z}^* + \text{c.c.}) \\ & + K_6\partial_z A_{\mu z}\partial_z A_{\mu z}^*. \end{aligned} \quad (17)$$

General expressions on the coefficients in the GL free energy are involved and will be presented in Appendix A. Here, their limiting behaviors in the limits of weak anisotropy, $\delta_u \rightarrow 0$, and of strong anisotropy, $|\delta_u| \rightarrow \infty$, will be explained together with their implication. In the case of a small $|\delta_u|$, β_z vanishes up to $O(|\delta_u|)$, and then the remaining GL coefficients of f_{bulk} reduce to those given in Ref. [2]. In the isotropic ($\delta_u \rightarrow 0$) limit, the four coefficients of f_{grad} , K_j ($j = 3, \dots, 6$), vanish, while K_1 and K_2 coincide with those given in Ref. [16]. Among them, K_1 logarithmically diverges upon cooling, reflecting the cancellation between the relaxation rate and the pairing vertex mentioned in Sec. II.

In contrast, in the $|\delta_u| \rightarrow \infty$ limit, the coefficients in f_{bulk} have the following limiting values:

$$\begin{aligned} \alpha & \simeq \frac{1}{3}N(0)\left[\ln\left(\frac{T}{T_{c0}}\right) + \psi\left(\frac{1}{2} + \frac{1}{8\tau T}\right) - \psi\left(\frac{1}{2}\right)\right], \\ \alpha_z & \simeq \frac{1}{3}N(0)\ln\left(\frac{T}{T_{c0}}\right), \\ \beta_3^{(0)} & = -2\beta_1^{(0)} \simeq \frac{\pi T}{15}N(0)\sum_{\varepsilon>0}\frac{1}{|\tilde{\varepsilon}_{\infty}|^3}, \\ \beta_2^{(0)} = \beta_4^{(0)} & = -\beta_5^{(0)} \simeq \beta_3^{(0)} - \frac{\pi^2 T}{60\tau}N(0)\sum_{\varepsilon>0}\frac{1}{\tilde{\varepsilon}_{\infty}^4}, \\ \beta_3^{(1)} & = -2\beta_1^{(1)} \simeq -\beta_3^{(0)} + \frac{\pi T}{15}N(0)\sum_{\varepsilon>0}\frac{1}{\varepsilon^2|\tilde{\varepsilon}_{\infty}|}, \\ \beta_2^{(1)} = \beta_4^{(1)} & = -\beta_5^{(1)} \simeq \beta_3^{(1)} + \frac{\pi^2 T}{60\tau}N(0)\sum_{\varepsilon>0}\frac{1}{\tilde{\varepsilon}_{\infty}^4}\left(1 - \frac{\tilde{\varepsilon}_{\infty}^2}{2\varepsilon^2}\right), \\ \beta_{12345}^{(0)} + 2\beta_{12345}^{(1)} + \beta_z & \simeq \frac{\pi T}{10}N(0)\sum_{\varepsilon>0}\frac{1}{|\varepsilon|^3}, \end{aligned} \quad (19)$$

where $\beta_{12345} = \beta_1 + \beta_2 + \beta_3 + \beta_4 + \beta_5$. It can be verified that $\beta_n^{(1)}$ and β_z vanish in the limit with no impurity scattering, i.e., when $\tau^{-1} = 0$.

The fact that α_z approaches its result for the bulk liquid in $|\delta_u| \rightarrow \infty$ is a consequence of the specular scattering along the polar axis [see Eq. (6)] and implies that the superfluid transition temperature T_c between the normal phase and the polar pairing state is not affected by the impurity scattering in the limit of strong anisotropy. Thus, this α_z -expression can be regarded as one analog of Anderson's theorem [17] in the s -wave superconductor [15,18,19]. Consistent with the behavior of α_z , the last line of Eq. (19), which is the coefficient of the quartic bulk term associated with the polar order parameter $A_{\mu z}$, also becomes independent of τ . Therefore, the mean-squared amplitude of the polar order parameter $|\Delta_{\text{polar}}|^2 = A_{\mu z}^*A_{\mu z}$, which becomes $-\alpha_z/[2(\beta_{12345}^{(0)} + 2\beta_{12345}^{(1)} + \beta_z)]$ within the present GL treatment, is also independent of τ [18–20]. Such an impurity-free nature associated with the polar pairing does not hold in the transition temperature to another pairing state at lower temperatures [15,19].

As will be discussed in detail elsewhere [19], the above-mentioned impurity-free thermodynamic behavior of the polar pairing state at finite temperatures is approximately satisfied beyond the GL approach as far as, say, $|\delta_u| \geq 10$. So, even for superfluid ^3He in aerogels to be modeled by a finite $|\delta_u|$, the model in the limit of strong anisotropy can be conveniently used for theoretical descriptions.

Due to the nonvanishing δ_u , as seen in Eq. (17), the quadratic gradient energy f_{grad} consists of the six invariants, and the corresponding six coefficients remain nonvanishing even in the limit of strong anisotropy ($|\delta_u| \rightarrow \infty$). In the low- T limit, all coefficients remain nonvanishing, and their leading terms in the low- T limit become

$$\begin{aligned} K_1 & \simeq \frac{\pi^2 T v^2}{120}N(0)\sum_{\varepsilon>0}\frac{1}{|\varepsilon|\tau|\tilde{\varepsilon}_{\infty}|^3}, \\ K_4 & \simeq \frac{\pi^2 T v^2}{48}N(0)\sum_{\varepsilon>0}\frac{1}{|\varepsilon|^2\tau|\tilde{\varepsilon}_{\infty}|^2}, \\ K_5 & \simeq \frac{\pi^2 T v^2}{480}N(0)\sum_{\varepsilon>0}\frac{1}{|\varepsilon|^2\tau|\tilde{\varepsilon}_{\infty}|^2}\left(1 + \frac{5}{4}\frac{\pi}{|\tilde{\varepsilon}_{\infty}|\tau}\right). \end{aligned} \quad (20)$$

Further, the coefficient of $\partial_z A_{\mu z}^*\partial_z A_{\mu z}$, which arises from the sum of the K_4 , K_5 , and K_6 terms, approaches

$$\frac{\pi^2 T v^2}{80}N(0)\sum_{\varepsilon>0}\frac{1}{\varepsilon^2\tilde{\varepsilon}_{\infty}^2\tau}. \quad (21)$$

The divergent behaviors $\sim \varepsilon^{-2}$ in the low- T limit of Eq. (21) correlate with the τ -independent $\sim -|\varepsilon|^{-1}$ behavior leading to the $|\ln T|$ contribution in α_z . In contrast, K_2 and K_3 reduce to finite values in the low- T limit.

IV. DESCRIPTION OF THE HQV PAIR IN THE PDB PHASE IN THE LONDON LIMIT

To correctly understand the order parameter structures of a HQV pair obtained numerically, it is useful to have an intuitive image of a HQV pair by describing it in the London limit where the order parameter $A_{\mu j}$ is described in terms of the angle variables while keeping the overall amplitude fixed.

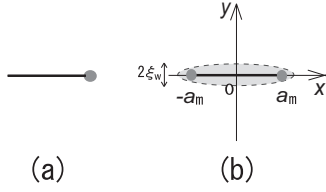


FIG. 2. (a) A single HQV (solid dot) in a B phase described in the x - y plane. To make the order parameter $A_{\mu,j}$ single-valued, its one component must vanish on the string (solid line). (b) A pair of HQVs in a B phase is accompanied by the string on which $A_{\mu,j}$ takes the form of the two-dimensional planar state. This planar string has a finite length $\simeq 2a_m$ and a width $2\xi_w$ if the two HQVs are well separated. In the double-core vortex in the bulk liquid, the string shrinks so that the planar pairing state is realized only close to the center of the vortex, i.e., the origin (see the discussion on Fig. 5 in Sec. V).

Hereafter, we focus on the HQV lines extended along the polar axis \hat{z} . Thus, the vortex lines will be described as point vortices on the 2D plane, and the KLS wall [7,10] (see Sec. I) connecting two separated HQVs with each other will be referred to as a string defect.

First, let us review how to describe a single HQV [8]. By expressing a relative rotation around the x -axis between the orbital and spin frames in terms of the rotation matrix $[R_x(\theta)]_{\mu\nu} = \hat{x}_\mu \hat{x}_\nu + \delta_{\mu\nu}^{(x)} \cos\theta - \varepsilon_{x\mu\nu} \sin\theta$, the order parameter in the PdB phase in an environment with a uniaxially stretched anisotropy is expressed following the notation in Ref. [21] as

$$\begin{aligned} A_{\mu j} &= |\Delta| e^{i\Phi} [R_x(\theta)]_{\mu\nu} \left(\frac{c}{\sqrt{2}} \delta_{\nu j}^{(z)} + \sqrt{1-c^2} \hat{z}_\nu \hat{z}_j \right) \\ &= \frac{|\Delta|}{\sqrt{2}} e^{i\Phi} \begin{pmatrix} c & 0 & 0 \\ 0 & c \cos\theta & -\sqrt{2(1-c^2)} \sin\theta \\ 0 & c \sin\theta & \sqrt{2(1-c^2)} \cos\theta \end{pmatrix} \end{aligned} \quad (22)$$

[see also Eq. (4) in Ref. [7]], where c ($0 \leq c \leq \sqrt{2/3}$) is the parameter playing the role of the order parameter of the PdB phase, $\delta_{\mu\nu}^{(x)} = \delta_{\mu\nu} - \hat{x}_\mu \hat{x}_\nu$, and the overall phase Φ was introduced. In the polar limit where $c \rightarrow 0$, Eq. (22) reduces to the order parameter of the polar phase with $d_\mu = \hat{z}_\mu \cos\theta - \hat{y}_\mu \sin\theta$ [6].

A single HQV localized at the origin is expressed by choosing $\Phi = \theta = \phi/2$. Then, the corresponding order parameter becomes

$$A_{\mu j} = \frac{|\Delta|}{\sqrt{2}} \left[c e^{i\phi/2} \hat{x}_\mu \hat{x}_j + \sqrt{1-\frac{c^2}{2}} (e^{i\phi} \hat{e}_{-\mu} \hat{e}'_{+j} + \hat{e}_{+\mu} \hat{e}'_{-j}) \right], \quad (23)$$

where the unit vectors $\hat{e}_{\pm\mu} = (\hat{y} \pm i\hat{z})_\mu / \sqrt{2}$ and $\hat{e}'_{\pm j} = [c\hat{y} \pm i\sqrt{2(1-c^2)}\hat{z}]_j / \sqrt{2-c^2}$ were introduced. The fact that only A_{xx} does not become a single-valued component upon circling the vortex center implies that, as sketched in Fig. 2(a), A_{xx} inevitably vanishes on a string corresponding to a branch cut with a fixed ϕ -value. In other words, a polar-distorted *planar* state is realized on the string [8,14].

The above expression of the order parameter in the London limit is easily generalized to the case with a HQV pair. Since

we should consider a HQV pair to be compared with the ordinary phase vortex with an integer winding number of the phase, the angle variables Φ and θ will be chosen in the manner

$$\Phi = \frac{\phi_+ + \phi_-}{2}, \quad \theta = \frac{\phi_+ - \phi_-}{2}, \quad (24)$$

where $\phi_\pm = \tan^{-1}[y/(x \mp a)]$. Then, Eq. (23) is replaced by Eq. (22) with Eq. (24), i.e.,

$$\begin{aligned} A_{\mu j} &= \frac{|\Delta|}{\sqrt{2}} \left[c e^{i(\phi_+ + \phi_-)/2} \hat{x}_\mu \hat{x}_j \right. \\ &\quad \left. + \sqrt{1-\frac{c^2}{2}} \left(e^{i\phi_+} \hat{e}_{-\mu} \hat{e}'_{+j} + e^{i\phi_-} \hat{e}_{+\mu} \hat{e}'_{-j} \right) \right]. \end{aligned} \quad (25)$$

In this case, sketched in Fig. 2(b), the expression of A_{xx} implies that the order parameter in $|x| > a$ is continuous through the x -axis, while the string is necessary in $|x| < a$. In relation to the results in Sec. V, it is valuable to point out that the solution of Eq. (24) on the y -axis is given by $\Phi = \pi/2$ and

$$\cos\theta = \left[1 + \left(\frac{a}{y} \right)^2 \right]^{-1/2}. \quad (26)$$

Next, the dependence of the HQV pair's energy on the HQV pair size $2a$ will be considered [8] using the gradient energy terms. The a -dependent contribution of the vortex energy will be denoted as $\Delta F_L(a) = F(a) - F(\xi_c)$, where ξ_c is a cutoff length corresponding to the core size of a HQV over which the London limit may be used. Since only the vortex lines extending along the z -axis are considered, the three gradient terms with coefficients K_3 , K_5 , and K_6 in Eq. (17) are neglected. Then, using Eq. (25), the contribution of Eq. (17) to $\Delta F_L(a)$ becomes

$$\Delta F_L^{(2)}(a) = -\frac{\pi}{2} c^2 |\Delta|^2 (K_1 + K_2) \ln \left(\frac{2a}{\xi_c} \right) \quad (27)$$

in a clean limit where $\tau^{-1} = 0$, $K_1 + K_2 \simeq 7\zeta(3)\xi_0^2 N(0) T_{c0}^2 / (30T^2)$, and $\xi_0 = v / (2\pi T_{c0})$. The two limiting forms of Eq. (27) are already known: Such an energy gain of the double-core vortex relative to the so-called α -vortex [22] in the bulk B phase is given by Eq. (27) with $c^2 = 2/3$ [8,16]. Further, the factor c^2 in Eq. (27) is consistent with the vanishing $\Delta F_L^{(2)}(a)$ in the opposite polar limit where $c = 0$ [6]. It can be checked that the nonvanishing Eq. (27) proportional to c^2 follows only from spatial variations of A_{xx} , which is absent in the polar phase.

As shown in Ref. [6], the negative $\Delta F_L(a)$ in the polar limit occurs only from the gradient term expressing the Fermi-liquid (FL) or spin-fluctuation correction. It is known [5] that, in the London limit, such a negative $\Delta F_L(a)$ for a HQV pair in the A phase occurs from a difference due to the FL correction between the superfluid density and the spin superfluid density. Within the framework based on the GL expansion, the gradient terms due to the FL correction arise

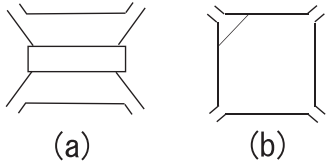


FIG. 3. (a) Diagram giving the FL correction to the gradient energy. The rectangle denotes the vertex part representing the renormalized interaction between the quasiparticles. (b) One example of a vertex correction to the weak-coupling quartic order term (Gor'kov box).

in $O(|\Delta|^4)$ terms sketched in Fig. 3(a) and, in a clean limit where $\tau^{-1} = 0$, they are given by [6]

$$\begin{aligned}
 f_{\text{FL}}^{(4)} = & \frac{N(0)}{450} \Gamma_1^s (\pi v)^2 \left(T \sum_{\varepsilon > 0} \frac{1}{\varepsilon^3} \right)^2 \{ (\nabla \cdot A_\mu) (\nabla \cdot A_\lambda^*) A_{\mu i}^* A_{\lambda i} \\
 & + (\nabla A_{\mu i}) \cdot (\nabla A_{\lambda j}^*) A_{\mu i}^* A_{\lambda j} + (A_\lambda \cdot \nabla) A_{\lambda i}^* (A_\mu^* \cdot \nabla) A_{\mu i} \\
 & - ((\nabla A_{\mu i}^*) \cdot (\nabla A_{\lambda j}^*)) A_{\mu i} A_{\lambda j} + (A_\mu \cdot \nabla) A_{\mu i}^* (A_\lambda \cdot \nabla) A_{\lambda i}^* \\
 & + (\nabla \cdot A_\mu^*) (\nabla \cdot A_\lambda) A_{\mu i} A_{\lambda i} + 2[(\nabla \cdot A_\mu) \\
 & \times [A_{\mu i}^* (A_\lambda \cdot \nabla) A_{\lambda i}^* + A_{\lambda i} (A_\mu^* \cdot \nabla) A_{\mu i}^*] \\
 & + A_{\mu i}^* [(A_\lambda \cdot \nabla) A_{\lambda i}^* \cdot \nabla] A_{\mu i} - ((\nabla \cdot A_\mu^*) [A_{\lambda i} (A_\mu \cdot \nabla) A_{\lambda i}^* \\
 & + A_{\mu i} (A_\lambda \cdot \nabla) A_{\lambda i}^*] + A_{\lambda i} [(A_\mu \cdot \nabla) A_{\mu i}^* \cdot \nabla] A_{\lambda i}^*] + \text{c.c.} \}, \\
 & (28)
 \end{aligned}$$

where ε is the fermion Matsubara frequency, and the spin-antisymmetric Landau parameter Γ_1^a was assumed to be negligibly small [5,6]. Applying Eq. (25) to Eq. (28), the corresponding contribution to $\Delta F_L(a)$ becomes

$$\begin{aligned}
 \Delta F_L^{(4)}(a) & \simeq \frac{c^{-2}}{30} \Gamma_1^s |\psi^{(2)}(1/2)|^2 \left(\frac{T c_0 |\Delta|}{\pi T^2} \right)^2 \Delta F_L^{(2)}(a) \\
 & \simeq -0.1 \pi \Gamma_1^s \left(\frac{T c_0 |\Delta|^2}{\pi T^2} \right)^2 \xi_0^2 N(0) \ln \left(\frac{2a}{\xi_c} \right), \quad (29)
 \end{aligned}$$

where the next-order terms of $O(c^2)$ were neglected. Here, $\psi^{(2)}(1/2) = -14\zeta(3)$, and $\Gamma_1^s = F_1^s / (1 + F_1^s/3)$ is the pressure-dependent constant of order unity with a Landau parameter $F_1^s (> 0)$. Thus, the energy gain corresponding to a repulsion between two HQVs composing a pair is dominated by the FL correction term rather than the ordinary weak-coupling terms in the strongly anisotropic PdB phase with a low enough $|c|$ -value.

In the present PdB phase, we also have an energy cost due to the KLS string (wall). This contribution due to the nonzero A_{xx} is estimated like

$$\Delta F_w(a) \simeq 0.1 N(0) \xi_0^2 |\Delta|^2 c^2 a / \xi(T), \quad (30)$$

where $\xi(T) = \xi_0 [N(0)/|\alpha|]^{1/2}$. The coefficient $\Delta F_w(a)/a$ measures the line tension of the string. By optimizing the sum $\Delta F_L^{(2)} + \Delta F_L^{(4)} + \Delta F_w$ with respect to a , the pair size to be realized is given by

$$2a_m \simeq c^{-2} \frac{2\Gamma_1^s}{\pi} \left(\frac{|\Delta|}{T} \right)^2 \xi(T). \quad (31)$$

In this way, it is expected in the London limit that the size of a HQV pair, a_m , i.e., the longer radius of the elliptical core of the double-core vortex, is a microscopic scale in the bulk B phase, while in a strongly anisotropic PdB phase close to T_{PB} where $|c| \ll 1$, the pair size may become a macroscopic one. This result will be used to discuss the content of our numerical results in the next section.

Since the GL free energy is written in the form of expanding in powers of the order-parameter field, it is not clear to what extent the results in GL theory are quantitatively reliable deep in the superfluid states. We expect that the present approach [6] has improved such a defect of the GL approach to superfluid ^3He by including the FL correction terms. In fact, if, as in the conventional GL approach [11,12,21–24], the FL-corrected gradient terms are neglected, no HQV pair is stabilized in the polar phase [6], and, even in the PdB phase, the size of an assumed HQV pair would remain microscopic so that the presence [7] of a macroscopic HQV pair in the PdB phase could not be naturally explained. As mentioned above, a macroscopic HQV pair can be realized in the PdB phase as a combined effect of a strong anisotropy *and* the FL correction to the gradient energy.

V. NUMERICAL ANALYSIS AND RESULTS

In our numerical study, the GL model we use consists of the three contributions to the free-energy density, f_{bulk} , f_{grad} , and the additional $O(|\Delta|^4)$ contributions $f_{\text{grad}}^{(4)}$. Before proceeding to discussing our numerical results, comments on the two contributions, sketched in Fig. 3, to $O(|\Delta|^4)$ gradient terms [6] should be given.

The contribution $f_{\text{FL}}^{(4)}$, given in Eq. (28) in the case of a clean limit, arises through the repulsive channel of the interaction between the quasiparticles. In the limit of strong anisotropy, the corresponding free energy density is given by replacing ε in Eq. (28) by $\tilde{\varepsilon}_\infty$. Although Eq. (28) does not include the anisotropy parameter δ_u explicitly, the anisotropy-induced vertex correction with $C_0 - 1$ as a coefficient is, as is explained in Appendix A, safely negligible even in the limit of strong anisotropy. Therefore, in the temperature range where $|\varepsilon| \gg 1/\tau$, Eq. (28) may be safely used for our numerical purposes.

Another contribution to $f_{\text{grad}}^{(4)}$ arises from the ordinary weak-coupling $O(|\Delta|^4)$ term, the so-called ‘‘Gor'kov box,’’ unaccompanied by a repulsive interaction between quasiparticles [see Fig. 3(b)]. This contribution includes all the terms including those expressed by C_{21} , B_0 , and ΔB in the vertex correction Λ_j . As is explained in relation to Fig. 7(a), however, these vertex corrections are also safely negligible. This has been concluded through the full numerical results, although it is already known [6] that these anisotropy-induced terms in the weak-coupling diagrams do not affect the resulting size of the HQV pair irrespective of the anisotropy value. Therefore, regarding $f_{\text{grad}}^{(4)}$ to be added to f_{bulk} and f_{grad} , its expression in the isotropic case, i.e., Eq. (52) in Ref. [6], has been used to obtain numerical results even in the case with a strong enough anisotropy.

To numerically examine how the double-core vortex in the PdB phase is stabilized in the form of a HQV pair, we follow

the same route as in other works where the HQV pair in equal-spin pairing states [6] and the double-core vortex in the B phase in the isotropic aerogel [16] have been studied. First, Eq. (25) is used as the initial condition for obtaining a HQV pair with the lowest energy at fixed values of the temperature and pressure. The London solution, Eq. (25), has a fixed size $2a$ of the HQV pair as a parameter. The variational equations of the GL free energy explained above are solved to obtain the solution minimizing the energy for each a -value according to the direct two-dimensional method [11], i.e., by assuming the vortices to be straight line objects extending along the z -axis. For each run of our computation, we have checked that the size of the HQV pair of the *resulting* double-core vortex solution almost coincides with the $2a$ value set initially. This means that, by using Eq. (25) as the initial condition, the vortex texture at the outer boundary under a fixed a -value is also kept fixed during each run. Thus, in examining the dependence of the vortex energy

$$\Delta F(a) = F(a) - F(0) \quad (32)$$

on the a -value introduced as the initial condition, this a can be identified with half of the resulting size of the HQV pair. Here, $\Delta F(a)$ corresponds to $\Delta F_L(a)$ introduced in the London limit. In the language of the vortices in the bulk B phase, $F(0)$ corresponds to the free energy of the so-called o -vortex [22]. As our numerical results for some δ_u -values, x and y dependences of each component of the order parameter $A_{\mu,j}$ of the vortex solution minimizing $\Delta F(a)$ will be presented together with $\Delta F(a)$ data hereafter. The τ^{-1} -value will be fixed to 0.13 (mK) throughout this work.

Regarding the system sizes in the x - y plane perpendicular to the polar axis, we have assumed in most of our computations that the system size in the x (y) direction is fixed to 24 (1.2) (μm) in the layout sketched in Fig. 2(b), i.e., by assuming a HQV pair growing along the x direction. Results in the case with a larger system size [2.4 (μm)] in the y direction will be commented on later for each $|\delta_u|$ -value. The pressure dependence of the system is incorporated through the bulk transition temperature T_{c0} and the Fermi velocity v [23]. The dimensionless strength of the impurity scattering is $(\tau T_{c0})^{-1}$, which is enhanced upon decreasing the pressure reflecting the pressure dependence of T_{c0} [16,24].

Throughout the present study, the dipole energy is not taken into account. The neglect of the dipole energy is justified in the case of weaker anisotropy where the resulting size of the core composed of a HQV pair is much smaller than the dipole length $\xi_D \sim 10$ (μm). In contrast, a HQV pair resulting from a strong enough anisotropy may have a size of the order of ξ_D over which the dipole energy affects spatial patterns of the θ -variable, defined in Eq. (22), in the PdB phase [7]. However, one will see below in this section that the London limit becomes a better description upon increasing the anisotropy. Then, one has only to take the dipole energy into account later by, in turn, choosing the London limit [7] as the starting model for description.

First, the $|\delta_u| = 0.05$ case is discussed as a typical example of superfluid ^3He in a *weakly anisotropic* aerogel. Figures 4(a) and 4(b) express the corresponding phase diagram and the a versus $\Delta F(a)$ curves at $T = 1.469$ (mK) close to T_{PB} and at 1.447 (mK) under a fixed pressure $P = 9$ (bar), while

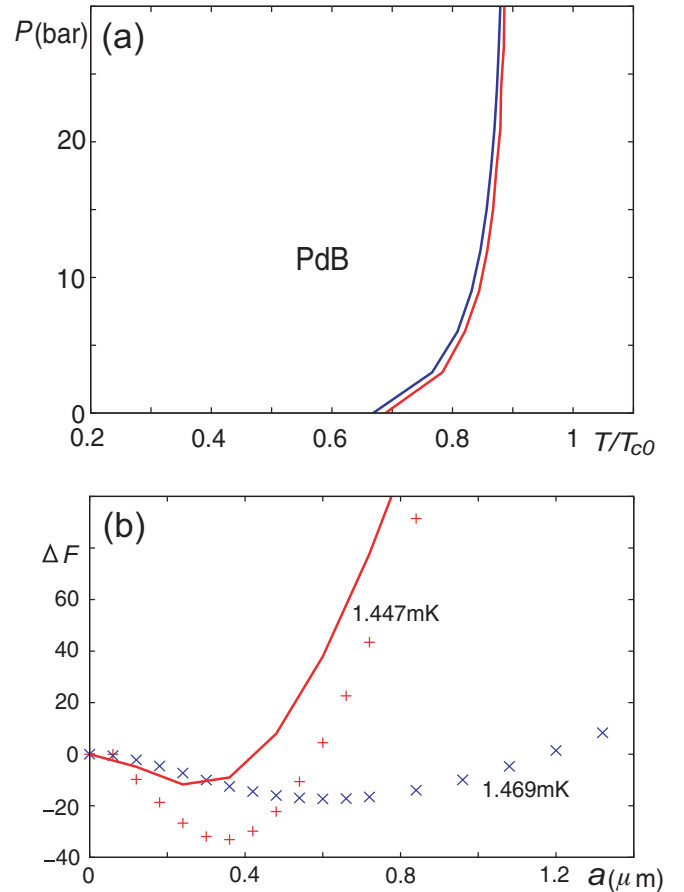


FIG. 4. Numerical results for $|\delta_u| = 0.05$. (a) P vs $T/T_{c0}(P)$ phase diagram, where $T_{c0}(P)$ is the superfluid transition line of the bulk liquid at each P . The red solid curve means the superfluid transition curve $T_c(P)$ between the polar and normal phases, while the blue curve denotes $T_{PB}(P)$ and is quite close to $T_c(P)$. (b) The a vs $\Delta F(a)$ curves at $P = 9$ (bar) and at $T = 1.447$ (mK) (red plus symbols) and 1.469 (mK) (blue cross symbols) close to T_{BP} . The a -value, a_m , minimizing $\Delta F(a)$ in the former is 0.38 (μm), while the corresponding one in the latter is 0.6 (μm) (see also Table I). For comparison, the corresponding curve at $T = 1.447$ (mK) obtained by neglecting the FL correction is shown by the solid red curve, which indicates $a_m = 0.24$ (μm).

Figs. 5(a) and 5(b) present spatial variations of each component of $A_{\mu,j}$ at $T = 1.469$ (mK) upon sweeping along the x and y axis, respectively. Here, the HQV pair is always assumed to be initially set as in Fig. 2(b), and the origin is

TABLE I. Resulting a_m values at different temperatures for various δ_u -values at 3 and 9 (bar). The c/c_M -value in each case is also shown, where $c_M = c(T = 0)$.

$ \delta_u $	0.05	0.05	4.4	4.4	4.4	300	300
P (bar)	9	9	9	3	3	3	3
T (mK)	1.447	1.465	1.28	0.815	0.8466	0.61	0.6396
c/c_M	0.628	0.403	0.391	0.369	0.094	0.363	0.157
a_m (μm)	0.36	0.48	0.54	0.9	5.28	1.02	6.24

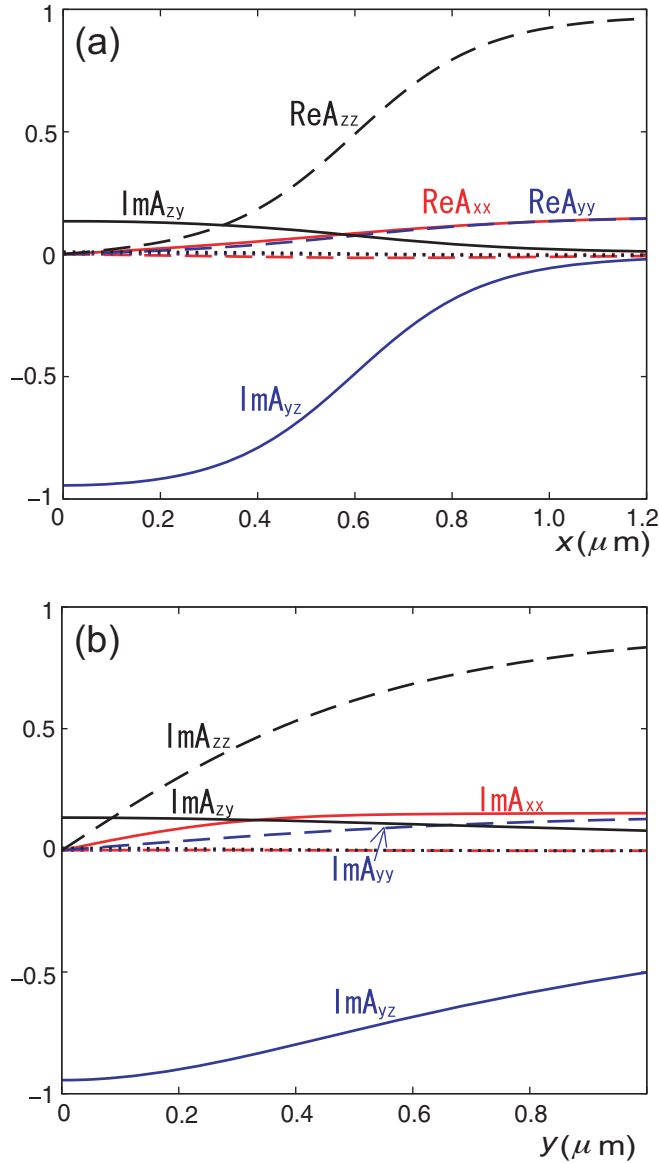


FIG. 5. Spatial variations of $A_{\mu j}$ components for $|\delta_u| = 0.05$ when sweeping (a) along the x -axis and at $y = 0$ at $a = a_m \simeq 0.6$ (μm) when $T = 1.469$ (mK) and $P = 9$ (bar), and (b) along the y -axis and at $x = 0$. Here, the vortex center is at $(0, 0)$. The $A_{\mu j}$ components other than the nonvanishing five components in the London representation, Eq. (22), are expressed by the dotted curves and a red dashed curve.

the center of the HQV pair. Furthermore, by symmetry, just the region in $x \geq 0$ and $y \geq 0$ is shown [6,11,12,16].

As Fig. 4(a) shows, the polar phase region in this $|\delta_u| = 0.05$ case is extremely narrow, and T_{PB} and T_c curves are quite close to each other. The decrease of T_c/T_{c0} at lower P is a consequence of $[\tau T_{c0}(P)]^{-1}$ increasing with decreasing P . In Fig. 4(b), the dependence of the vortex core energy ΔF on the initial value $2a$ of the HQV pair size is presented for the two values of $c(T)$. As Fig. 6(b) shows, the parameter $c(T)$ playing the role of the order parameter in the PdB phase grows upon cooling. The $2a$ value minimizing ΔF corresponds to the HQV pair size $2a_m$ to be realized. Closer to the phase boundary T_{PB} at which c vanishes, the a_m

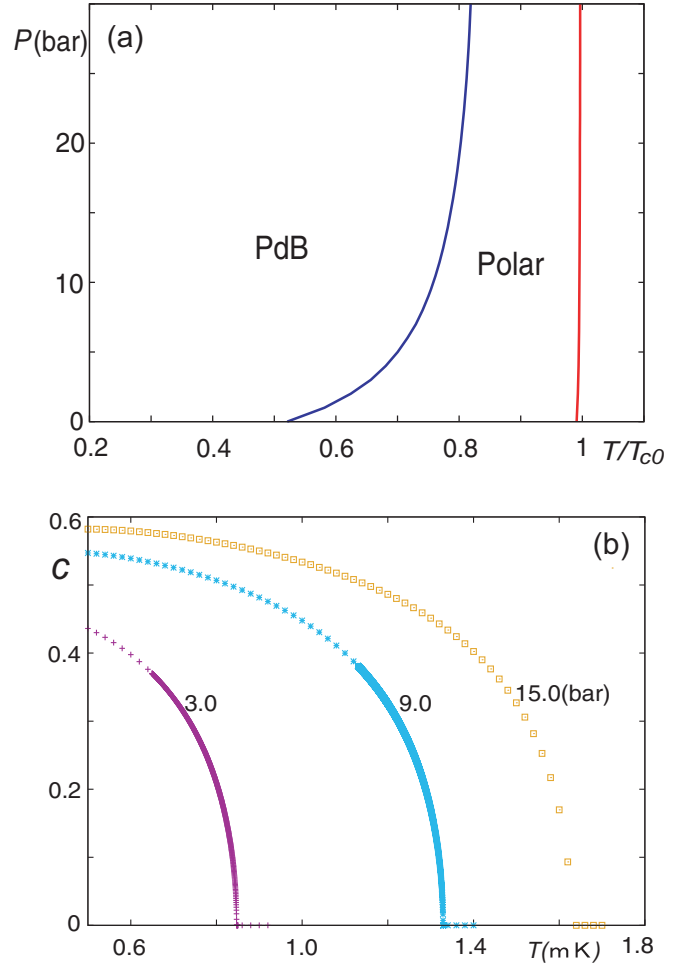


FIG. 6. Numerical results for $|\delta_u| = 4.4$. (a) Pressure P vs $T/T_{c0}(P)$ phase diagram. The red curve denotes the superfluid transition curve $T_c(P)$ between the polar and normal phases, and the blue curve denotes T_{PB}/T_{c0} . No remarkable shift of T_c from T_{c0} is seen. (b) Temperature dependence of the “order parameter” c in the PdB phase at the pressures $P = 3.0$ (bottom), 9.0 , and 15.0 (top) (bar).

value becomes divergent as suggested by Eq. (31). Further, as the solid curve in Fig. 4(b) shows, the conventional GL free energy with no FL correction term, Eq. (28), results in a smaller size $2a_m = 0.48$ (μm) of the HQV pair [9,16]. Such a correlation-induced growth of the HQV pair size has been pointed out elsewhere [9,16]. Further, although we have also performed the computation using a larger system size [2.4 (μm)] in the y direction, the obtained results have shown no size dependence.

Figures 5(a) and 5(b) show spatial variations of $A_{\mu j}$ upon sweeping along the x and y axis, respectively, for $c = 0.2$ and $|\delta_u| = 0.05$. Broadly speaking, the midpoints of the A_{yz} and A_{zz} curves in Fig. 5(a) correspond to the position of the HQV, i.e., $x = a_m$. In the isotropic case where $c^2 = 2/3$ irrespective of the temperature, $|A_{yz}|$ and $|A_{zy}|$ at the origin coincide with each other. A large difference between them at $x = 0$ appears in Fig. 5 due to the “anisotropy” value, $c = 0.2$. This can be understood from Eq. (22) with $\phi_+ = \pi$ and $\phi_- = 0$. Upon approaching the vortex center along the x -axis, A_{xx} decreases. However, A_{xx} seems to be nonvanishing even close to $x = 0$.

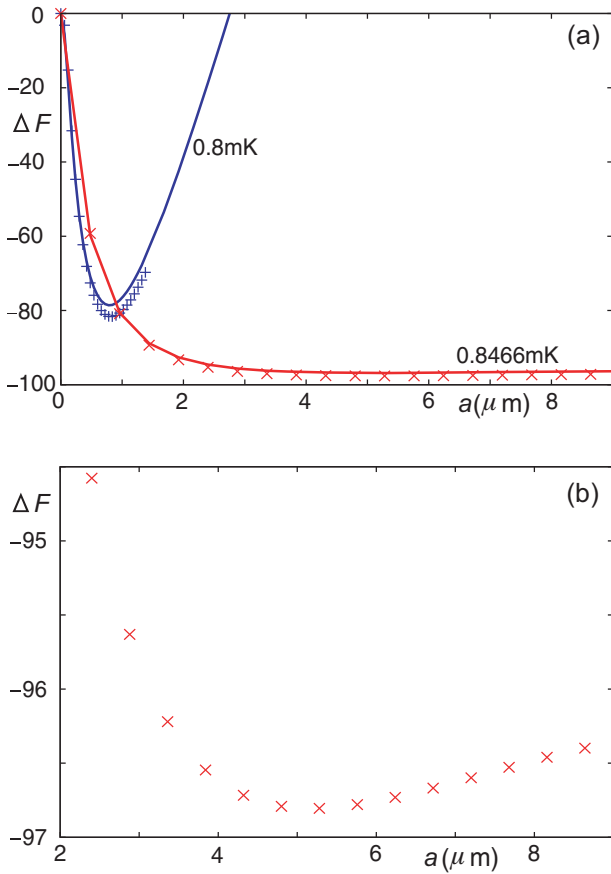


FIG. 7. Numerical results for $|\delta_u| = 4.4$ at 3 (bar). In (a), the a vs $\Delta F(a)$ curves are expressed by the blue solid curve at 0.8 (mK) and by the red solid curve at 0.8466 (mK) close to T_{PB} , and they have $a_m = 0.78$ (μm) and 5.28 (μm), respectively. For comparison, the results (plus and crossed symbols) in the case with additional vertex corrections (see the text) are also shown. Part (b) is the extended view of the red symbols around $a = 5.28$ in (a).

This means that, as in the bulk liquid, the polar-distorted planar state is realized only in the close vicinity of the origin (see also the caption of Fig. 2). Further, according to Fig. 5(b), the width ξ_w indicated in Fig. 2(b), i.e., the range of y over which A_{xx} linearly decreases, is large ($\simeq 0.3$). These behaviors of A_{xx} imply that, in spite of a substantial size $2a_m$ [$\simeq 1.2$ (μm)] of the HQV pair (see Table I), the core structure of the double-core vortex for $|\delta_u| = 0.05$ is similar to that of the bulk liquid. On the other hand, we note that, as Fig. 5(b) indicates, the y dependences of the four order-parameter components except A_{xx} are slow and seem to be consistent with Eqs. (22) and (26) following from the London limit.

Next, the corresponding results in a case with a moderately strong anisotropy, $|\delta_u| = 4.4$, are presented in Figs. 6 and 7. The P - T phase diagram and the temperature dependence of the order parameter c of the PdB phase are given in Figs. 6(a) and 6(b), respectively. Figure 6(a) shows that a moderately wide region of the polar phase is realized in this case. The feature that T_c/T_{c0} is almost P -independent and takes values close to unity at any P indicates that the $|\delta_u| = 4.4$ case is not far from the limit of strong anisotropy in which Anderson's theorem is strictly valid [15].

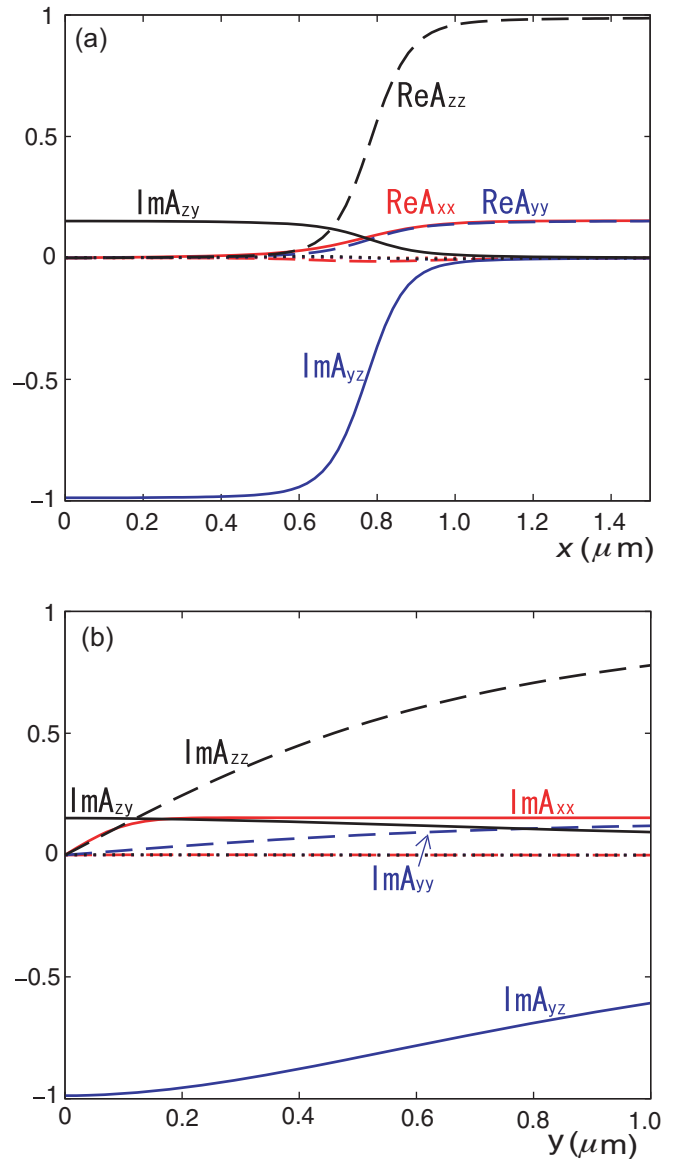


FIG. 8. Part (a) expresses the data, at $a = a_m = 0.78$ of the blue solid curve in Fig. 7(a), of spatial variations of $A_{\mu j}$ components on sweeping along the x -axis and at $y = 0$. Part (b) corresponds to (a) on sweeping y and at $x = 0$. Here, the vortex center is at $(0,0)$.

In Figs. 7(a) and 8, we focus on the $P = 3$ (bar) case and on the results at the two temperatures, 0.8466 (mK) at which $c = 0.0456$ (or $c/c_M \simeq 0.094$) and 0.8 (mK) at which $c = 0.214$ (or $c/c_M \simeq 0.439$), where $c_M(P)$ is the c value in the $T \rightarrow 0$ limit at each pressure. Figures 8(a) and 8(b) express the spatial variations of the components of $A_{\mu j}$ at 0.8 (mK) in $P = 3$ (bar) when $|\delta_u| = 4.4$. Some clear differences between Figs. 8(a) and 5(a) are seen. First, in the notation of Eq. (25), the following relations are satisfied in Fig. 8(a); $\theta \simeq 0$ and $|A_{xx}| \simeq c/\sqrt{2}$ in $x > a_m$, while $\theta \simeq \pi/2$ and $|A_{xx}| = 0$ in $0 \leq x < a_m$. Next, the linearly vanishing behavior of A_{xx} (red solid curve) upon lowering $|y|$ and at $x = 0$ is seen only in a narrow region of about 0.1 (μm) near the origin. In addition, the linear behavior $\Delta F(a) \propto a$ is nicely seen in $a > a_m$ in Figs. 7(a) and 7(b). These features lead to the conclusion that

the (polar-distorted) planar string is well-defined and has a length comparable with the size $2a_m$ of the HQV pair. In fact, Figs. 7(a) and 7(b) show that such a linear behavior approximately obeys the relation $S(T)c^2a$ where the T -dependent coefficient $S(T)$ slowly increases upon cooling, i.e., a relation consistent with the London result, Eq. (31). Furthermore, except in the vicinity of each HQV, other components of $A_{\mu j}$ than the five nonvanishing ones in Eq. (22) can be regarded as being zero.

Based on these features, in contrast to the $|\delta_u| = 0.05$ case, the double-core vortex for $|\delta_u| = 4.4$ is consistent with the description in the London limit and can be regarded as a well-defined HQV pair. Its origin seems to consist in the simple structure of the HQV in the $c \rightarrow 0$ limit, i.e., in the polar phase. As shown in Ref. [6], the spatial variations of the order parameter are surprisingly simple and are well represented by Eq. (25) with $c = 0$ and $A_{xx} = 0$ except in the close vicinity of each HQV. A smaller c -value effectively implying a stronger anisotropy leads to a structure closer to that in the London limit. In Fig. 7(a), we have also presented the $\Delta F(a)$ versus a curves (plus and crossed symbols) in the case where the $O(|\Delta|^4)$ gradient energy includes all of the vertex corrections accompanied by C , B , and D in Eq. (8). The deviation from the case with no such vertex corrections in the $O(|\Delta|^4)$ gradient energy is negligibly small, and the resulting a_m value is not affected much by including such vertex corrections. Therefore, we judge that the neglect of the vertex corrections to the $O(|\Delta|^4)$ gradient terms, mentioned in the beginning of this section, is valid in all of the other results presented here.

We have also examined how the obtained results are changed using larger system sizes, and we found a size dependence of the resulting HQV pair size. First, the use of a larger system size in the x -direction does not change the results in this section. In contrast, the size $2a_m$ of a HQV pair in $|\delta_u| = 4.4$ and 300 cases is *increased* 1.15 times when the system size in the y direction is 2.4 (μm), which is twice the corresponding size used in the figures in this section. Such a size dependence is never seen for $|\delta_u| = 0.05$. The size dependence mentioned above does not change our conclusion that, as the anisotropy is increased, the core structure of the double-core vortex in the bulk B phase is changed to a simple HQV pair consistent with the description in the London limit. In fact, the spatial variations of the $A_{\mu j}$ components shown in Figs. 8 and 9 are not affected qualitatively by the change of the system size in the y direction.

The corresponding results for a much stronger anisotropy, $|\delta_u| = 300$, are given in Fig. 9. Figures 9(a) and 9(b) express spatial variations of $A_{\mu j}$ for $|\delta_u| = 300$. Here, to examine the anisotropy dependences of the obtained results at the same pressure, we have compared the results at the same value of $c(T)/c_M$ with each other, because $c(T)/c_M$ seems to become a common measure of the distance in the phase diagram from T_{PB} at a fixed P (see also the next paragraph). Surprisingly, Fig. 9 is qualitatively similar to Fig. 8, suggesting that the $|\delta_u| = 4.4$ case is already close to the limit of the strong anisotropy. Nevertheless, as can be seen in Table I, the resulting size a_m of the HQV pair minimizing the energy at the same pressure and at the same c/c_M -value slightly increases upon increasing the anisotropy $|\delta_u|$. This is understood as a

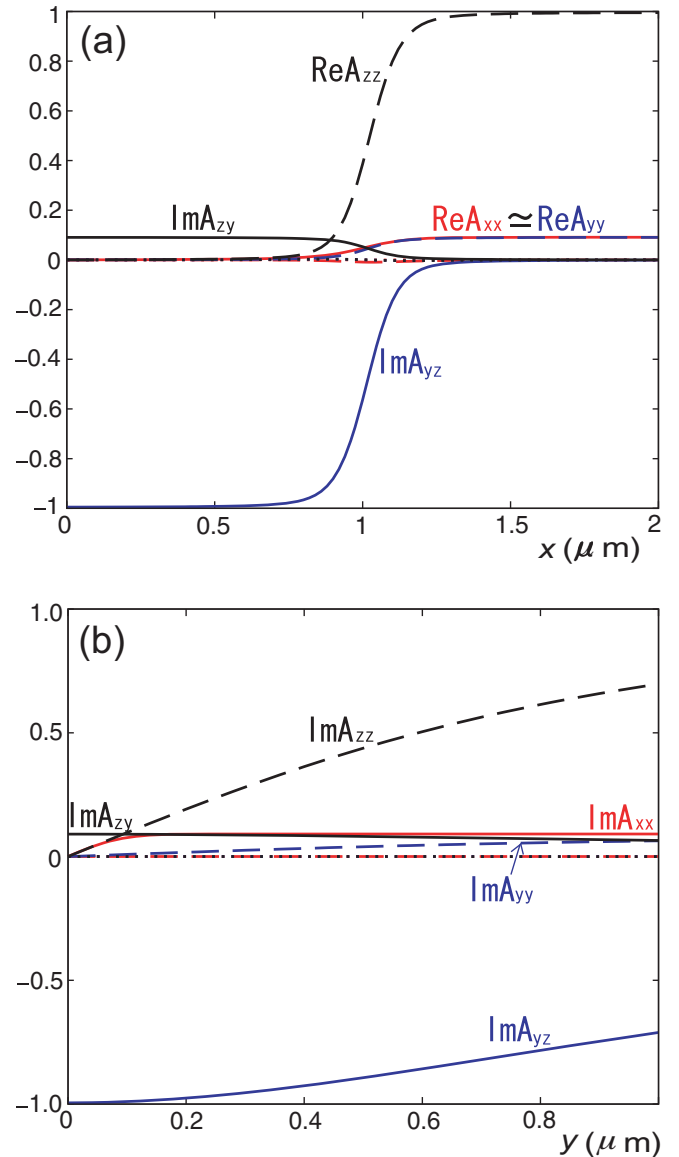


FIG. 9. (a) Spatial variations of $A_{\mu j}$ at 0.61 (mK) (or $c = 0.127$) below T_{PB} at 3 (bar) for $|\delta_u| = 300$ obtained on sweeping along the x axis and at $y = 0$. (b) Corresponding results to (b) taken along the y axis and at $x = 0$.

result of a weak temperature dependence of the amplitude of the order parameter when noting that Eq. (31) can be rewritten in the form

$$a_m \propto c_M^{-2} \left(\frac{T_c}{T} \right)^2 \sqrt{1 - \frac{T}{T_c}} \quad (33)$$

at a fixed pressure and fixed c/c_M -value, and that, when $|\delta_u| = 4.4$, the c_M -value is already close to its value for $|\delta_u| = 300$. In Table I, we have also shown the pressure dependences of the resulting a_m value. The results in $P = 3$ (bar) and 9 (bar) at a fixed c/c_M value show the tendency that the obtained a_m becomes smaller with increasing P . As mentioned above, however, the obtained a_m -value is likely to be underestimated due to the smallness of the system size in the y -direction used in our computation. Thus, it is not clear to what extent the

TABLE II. Resulting thickness ξ_w of the KLS wall obtained based on the definition given in the text and for the same values as in Table I of the temperature, $|\delta_u|$ -value, and the pressure.

$ \delta_u $	0.05	0.05	4.4	4.4	4.4	4.4	300	300
P (bar)	9	9	9	9	3	3	3	3
T (mK)	1.447	1.465	1.28	1.33	0.815	0.8466	0.61	0.6396
c/c_M	0.628	0.403	0.391	0.058	0.369	0.094	0.363	0.157
ξ_w (μm)	0.2	0.278	0.073	0.121	0.108	0.226	0.092	0.299

present numerical results on the a_m -value are quantitatively reliable.

VI. SUMMARY

In this work, we have numerically examined the stability of a HQV pair in the PdB phase of superfluid ^3He in a strongly anisotropic aerogel by assuming the weak-coupling approximation and based on the hypothesis that the double-core vortex in the bulk B phase corresponds to the HQV pair detected in the PdB phase. Due to the weak-coupling approximation, the presence of the PdA phase in real systems is neglected, and the transition between the PdB and the polar phases becomes inevitably continuous in the present analysis. However, such a continuous transition is found at low enough pressures in real systems [25], and in this sense the present results may be directly applicable to the experimental situations.

Our main result in the present work is that the double-core vortex [11,12] in the PdB phase under a strong anisotropy can be regarded as a HQV pair described in the London limit, reflecting the fact that the HQV in the pure polar phase is well described in the London limit [6]. We expect based on this result that a HQV pair detected in the real PdB phase is not induced but just supported by the vortex pinning effect.

In Fig. 10, the color maps expressing the spatial distribution of the squared amplitude of the order parameter $\sum_{\mu,j} |A_{\mu,j}|^2$ are presented for different anisotropy values. In $|\delta_u| = 0.05$ (top figure), the two HQVs are tightly bound by a negligibly short planar string (wall), and the two HQVs accompanied by a broad region with a diminished amplitude of the order parameter are realized. In contrast, for larger anisotropies such that $|\delta_u| = 4.4$ and 300, the two HQVs take the form connected only by a thin polar-distorted planar string on which the amplitude of the order parameter is faintly diminished, and the core size of each HQV is diminished upon increasing the anisotropy. In this manner, the description in the London limit becomes better upon increasing the anisotropy.

Here, the present result will be compared with the experimental result in Ref. [7], where the HQV pairs in the PdB phase have been detected. To understand the structure of the resulting HQV pair better, we have estimated the width of the polar-distorted planar string ξ_w [see Fig. 2(b)]. Broadly speaking, this length is estimated by comparing the mass term and the gradient one of $O(A_{xx}^2)$ with each other, to be of the order of $\xi(T)/c$ [7,8]. From the numerical data, ξ_w will be defined by assuming that the y dependence of A_{xx} close to the origin is approximated by $c \tanh(y/\xi_w)/\sqrt{2}$ [7] [see also Eq. (22)]. As shown in Table II, ξ_w indeed grows

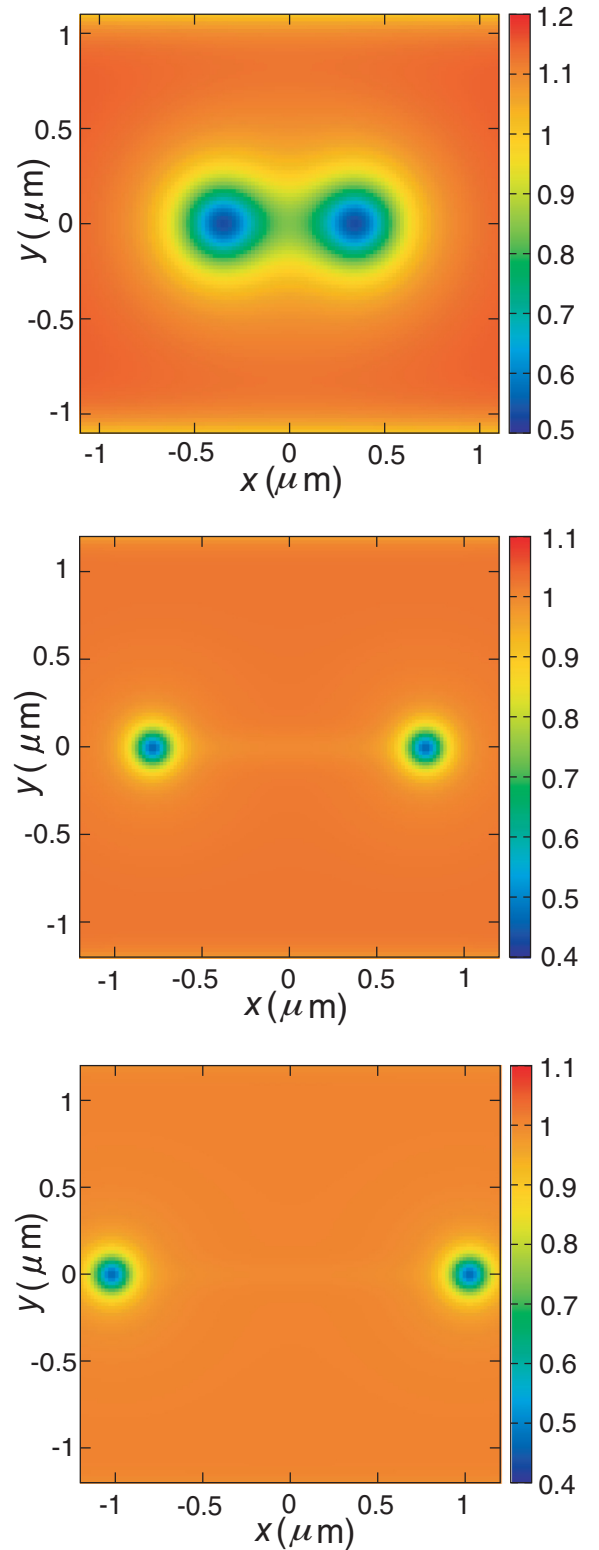


FIG. 10. Spatial profiles of the squared amplitude of the order parameter, i.e., $\sum_{\mu,j} |A_{\mu,j}|^2$ in the x - y plane in the cases of $|\delta_u| = 0.05$ (top), $|\delta_u| = 4.4$ (middle), and $|\delta_u| = 300$ (bottom). The c -value is 0.5 in the top figure. The middle figure corresponds to Fig. 8, while the bottom one corresponds to Fig. 9. A dim string representing the KLS wall connecting the two HQVs is seen in the middle and bottom figures, and the core size of each HQV is found to become smaller with increasing $|\delta_u|$.

with decreasing c/c_M . This is roughly consistent with the c^{-1} dependence mentioned above. On the other hand, the $|\delta_u|$ dependence of ξ_w is not anticipated easily and is found only through the present numerical analysis. Tables I and II suggest that, upon increasing the anisotropy $|\delta_u|$, the aspect ratio $2a_m/\xi_w$ becomes large enough to make the polar-distorted planar string a rigid and well-defined object. We note that this ratio is inversely proportional to $c(T)$, reflecting the proximity to the polar phase in which the size of a HQV pair is infinitely long in the present analysis where the dipole energy has been neglected.

The results on the vortex energy shown in Figs. 4 and 7 imply together with the data in Table I that the size of the HQV pair, a_m , is highly sensitive to the c -value. On the other hand, according to Ref. [7], huge HQV pairs have appeared in the PdB phase in spite of a reasonable T dependence of c corresponding to $\sqrt{2}q$ there [see the supplementary Fig. 5 in Ref. [7], which is qualitatively comparable with the present Fig. 6(b)]. It is evidence of the presence of a strong pinning in nematic aerogels keeping the size of a HQV pair significantly large [7].

In the experiment under rotation [1], the rotation axis has been fixed to the anisotropy (polar) axis, which is the z -direction in our notation. Furthermore, as mentioned above, the vortices created under a rapid quench [7] are also pinned along the polar axis because, due to the anisotropy, the coherence length is *effectively* the longest in this direction. Thus, it is possible that, if the aerogel is rotated with a rotation axis *perpendicular* to the polar axis, a pinning of the resulting vortices to the aerogel structure may be avoided. Then, the shrinkage of the HQV pair upon cooling might be observed in such a situation. There is another motivation regarding a study of HQVs extending along a direction perpendicular to the polar axis. Recently, NMR measurements for ^3He in a nematic aerogel squeezed by 30% in a direction perpendicular to the polar axis have been reported [26]. There, it has been found that the l -vector in the chiral PdA phase is largely directed along the squeezed direction. In this situation, the Majorana fermions may remain stable [27] in the core of a HQV in the PdA phase. For these reasons, it will be valuable to extend the present study on HQVs to the situation with the vortex axis perpendicular to the polar axis.

ACKNOWLEDGMENTS

One of the authors (R.I.) is grateful to V. V. Dmitriev and W. P. Halperin for useful discussions, and T. Hisamitsu for his help in obtaining Fig. 6(a). The present work was supported by JSPS KAKENHI (Grant No. 16K05444).

APPENDIX A

In this Appendix, details of the pairing vertex correction due to the impurity scattering and of the coefficient of each term in the resulting GL free energy are explained.

The impurity scattering potential does not carry the Matsubara frequency, and consequently, the corresponding self-energy term can be incorporated through the replacement of

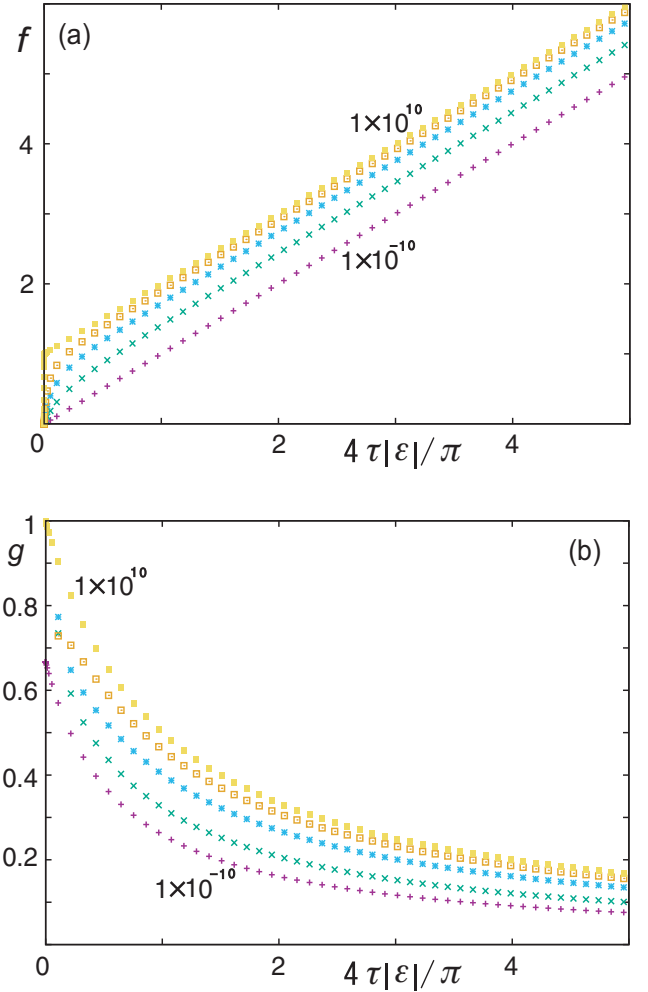


FIG. 11. (a) $f \equiv XC_0$ vs X curves for $|\delta_u| = 1 \times 10^{10}$ (top), 300, 30, 4.4, and 1×10^{-10} (bottom), where $X = 4\tau|\varepsilon|/\pi$. Note that f obeys $1 + X$ in $|\delta_u| \rightarrow \infty$, while it approaches X in the $\delta_u \rightarrow 0$ limit. (b) $g \equiv \pi X B_0/\tau$ vs X curves corresponding to those in (a). In $|\delta_u| \rightarrow \infty$, g obeys $1/(1 + X)$, while it approaches $2/[3 + \pi X/2]$ in $\delta_u \rightarrow 0$ in agreement with Eq. (9).

the Matsubara frequency $|\varepsilon|$ with

$$\begin{aligned} |\tilde{\varepsilon}_p| &= |\varepsilon| + \frac{1}{2\tau} \langle w(p - p') \rangle_{p'} \\ &= |\varepsilon| + \frac{1 + (|\delta_u|^{-1/2} - 1)\Theta(1 - |\delta_u|)}{4\tau} \\ &\quad \times \{ \tan^{-1}[|\delta_u|^{1/2}(1 - p)] + \tan^{-1}[|\delta_u|^{1/2}(1 + p)] \} \quad (\text{A1}) \end{aligned}$$

($|p| < 1$), where $p = \mathbf{p} \cdot \hat{z}/p_F$, and $\langle \rangle_p$ implies the average over the polar angle $\cos^{-1}(p)$.

The coefficients composing the vertex part Λ are given in the form

$$\begin{aligned} &\begin{pmatrix} B_0 & D_0 \\ \Delta B & \Delta D \end{pmatrix} \\ &= \frac{1}{2} \begin{pmatrix} 1 - I_{d11} & -|\delta_u|^{-1}(I_{d10} - I_{d11}) \\ -|\delta_u|(3I_{d12} - 4I_{d13}) & 1 - 3I_{d11} + 7I_{d12} - 4I_{d13} \end{pmatrix}^{-1} \\ &\quad \times \begin{pmatrix} e_1 & -I_{d21} + 2|\delta_u|^{-1}C_0(I_{d20} - I_{d21}) - e_1 \\ e_2 & 2C_0(3I_{d21} - 7I_{d22} + 4I_{d23}) - e_2 \end{pmatrix}, \quad (\text{A2}) \end{aligned}$$

where

$$e_1 = I_{d21} + |\delta_u|^{-1}(I_{d21} - I_{d20}), \quad (\text{A3})$$

$$e_2 = |\delta_u|(3I_{d22} - 4I_{d23}) - 3I_{d21} + 7I_{d22} - 4I_{d23}, \quad (\text{A4})$$

and

$$C_0 = \frac{1}{d},$$

$$C_{21} = \frac{-I_{d31} + I_{d32} + |\delta_u|^{-1}(I_{d30} - 2I_{d31} + I_{d32})}{d^2},$$

$$C_{1z} = 2dC_{21} - \frac{2}{d}[B_0(I_{d21} - I_{d22}) + \Delta B(I_{d20} - 2I_{d21} + I_{d22})], \quad (\text{A5})$$

$$C_{2z} = \frac{1}{d}[(2 + C_0)(I_{d31} - I_{d32}) - 2D_0(I_{d21} - I_{d22})] - \frac{1}{d|\delta_u|}[(2 + 3C_0)(I_{d30} - 2I_{d31} + I_{d32}) + 2\Delta D(I_{d20} - 2I_{d21} + I_{d22})].$$

Further,

$$d = 1 - 2(I_{d11} - I_{d12}),$$

$$I_{dmn} = \left\langle \frac{1 + (\sqrt{|\delta_u|} - 1)\Theta(|\delta_u| - 1)}{(2|\tilde{\varepsilon}_p|^m \tau (1 + |\delta_u|p^2)^n)} \right\rangle_p. \quad (\text{A6})$$

Among these coefficients, the $|\varepsilon|$ dependences of $C_0 - 1$ and B_0 are presented in Figs. 11(a) and 11(b), respectively. Here, $f = XC_0$, $g = \pi XB_0/\tau$, and $X = 4\tau|\varepsilon|/\pi$. Broadly speaking, the functions f and g decrease with decreasing $|\delta_u|$ -values. Since, more or less, we focus on the temperature range in which $2\tau|\varepsilon| \gg 1$, any impurity-induced vertex corrections become negligible in our numerical analysis.

Next, the coefficients in the GL free energy are given by

$$\alpha = \frac{1}{3}N(0) \left[\ln\left(\frac{T}{T_{c0}}\right) + 2\pi T \sum_{\varepsilon>0} \left(\frac{1}{|\varepsilon|} - \frac{3}{2}(I_{10} - I_{11}) \right) \right],$$

$$\alpha_z = \frac{1}{3}N(0) \left[\ln\left(\frac{T}{T_{c0}}\right) + 2\pi T \sum_{\varepsilon>0} \left(\frac{1}{|\varepsilon|} - 3I_{11}C_0 \right) \right], \quad (\text{A7})$$

where

$$I_{mn} = \left\langle \frac{p^{2n}}{|\tilde{\varepsilon}_p|^m} \right\rangle_p, \quad (\text{A8})$$

$$\beta_3^{(0)} = -2\beta_1^{(0)} = \frac{\pi T}{8}N(0) \sum_{\varepsilon>0} (I_{30} - 2I_{31} + I_{32}),$$

$$\beta_2^{(0)} = \beta_4^{(0)} = -\beta_5^{(0)} = \beta_3^{(0)} - \frac{\pi T}{64\tau}N(0) \int_{-1}^1 dp_1 \int_{-1}^1 dp_2 \sum_{\varepsilon>0} \frac{(1-p_1^2)(1-p_2^2)}{\tilde{\varepsilon}_{p_1}^2 \tilde{\varepsilon}_{p_2}^2 [1 + |\delta_u|(p_1 - p_2)^2]}$$

$$\times [1 + (\sqrt{|\delta_u|} - 1)\Theta(|\delta_u| - 1)],$$

$$\beta_z = -\frac{3}{2}(\beta_3^{(0)} + 2\beta_3^{(1)}) + \frac{\pi T}{2}N(0) \sum_{\varepsilon>0} C_0^4 I_{32} - \frac{\pi T}{64\tau}N(0)$$

$$\times \int_{-1}^1 dp_1 \int_{-1}^1 dp_2 \sum_{\varepsilon>0} \frac{(1-p_1^2 - 2p_1^2 C_0^2)(1-p_2^2 - 2p_2^2 C_0^2)}{\tilde{\varepsilon}_{p_1}^2 \tilde{\varepsilon}_{p_2}^2 [1 + |\delta_u|(p_1 - p_2)^2]} [1 + (\sqrt{|\delta_u|} - 1)\Theta(|\delta_u| - 1)],$$

$$\beta_3^{(1)} = -2\beta_1^{(1)} = -\beta_3^{(0)} + \frac{\pi T}{2}N(0) \sum_{\varepsilon>0} C_0^2 (I_{31} - I_{32}),$$

$$\beta_2^{(1)} = \beta_4^{(1)} = -\beta_5^{(1)} = \beta_3^{(1)} + \frac{\pi T}{64\tau}N(0)$$

$$\times \int_{-1}^1 dp_1 \int_{-1}^1 dp_2 \sum_{\varepsilon>0} \frac{(1-p_1^2)(1-p_2^2 - 2p_2^2 C_0^2)}{\tilde{\varepsilon}_{p_1}^2 \tilde{\varepsilon}_{p_2}^2 [1 + |\delta_u|(p_1 - p_2)^2]} [1 + (\sqrt{|\delta_u|} - 1)\Theta(|\delta_u| - 1)], \quad (\text{A9})$$

$$K_2 = \frac{\pi T v^2}{16}N(0) \sum_{\varepsilon>0} (I_{32} - 2I_{31} + I_{30}), \quad (\text{A10})$$

$$K_3 = \frac{\pi T v^2}{16}N(0) \sum_{\varepsilon>0} (-5I_{32} + 6I_{31} - I_{30}), \quad (\text{A11})$$

$$K_1 = K_2 + \frac{\pi T v^2}{4}N(0) \sum_{\varepsilon>0} [(I_{20} - I_{21})B_0 + (I_{21} - I_{22})\Delta B], \quad (\text{A12})$$

$$K_4 = -K_2 + \frac{\pi T v^2}{4}N(0) \sum_{\varepsilon>0} [(I_{31} - I_{32})C_0 - 8I_{11}C_{21}], \quad (\text{A13})$$

$$K_5 = 2K_3 + \frac{\pi T v^2}{8}N(0) \sum_{\varepsilon>0} [(3I_{21} - I_{20})B_0 + (3I_{22} - I_{21})\Delta B$$

$$+ (I_{20} - I_{21})D_0 + (I_{21} - I_{22})\Delta D + 2(I_{31} - I_{32})(C_0 - 1) - 8I_{11}C_{1z}],$$

$$\begin{aligned}
K_6 = & -7K_3 + \frac{\pi T v^2}{4} N(0) \sum_{\varepsilon > 0} [(3I_{21} - I_{20})D_0 \\
& + (3I_{22} - I_{21})\Delta D + (5I_{32} - 3I_{31})(C_0 - 1) - 8I_{11}C_{2z} \\
& + 3I_{31} - I_{30}]. \tag{A14}
\end{aligned}$$

APPENDIX B

Here, the possible effects of the pairing vertex correction, peculiar to the anisotropic scattering, on the $O(|\Delta|^4)$ gradient

$$\begin{aligned}
f_{\text{FL1}}^{(4)} = & \frac{N(0)}{225} \Gamma_1^s (\pi v)^2 \left[\left(T \sum_{\varepsilon > 0} \frac{1}{\varepsilon^3} C_0 \right)^2 \left[(\nabla \cdot A_\mu) (\nabla \cdot A_\lambda^*) A_{\mu z}^* A_{\lambda z} + (A_\lambda \cdot \nabla) A_{\lambda z}^* (A_\mu^* \cdot \nabla) A_{\mu z} \right] \right. \\
& + \left(T \sum_{\varepsilon > 0} \frac{1}{\varepsilon^3} \right) \left(T \sum_{\varepsilon > 0} \frac{1}{\varepsilon^3} C_0^2 \right) \left[\sum_{j=x,y} (\nabla A_{\mu z}) \cdot (\nabla A_{\lambda j}^*) A_{\mu z}^* A_{\lambda j} + \text{c.c.} \right] + \left(T \sum_{\varepsilon > 0} \frac{1}{\varepsilon^3} C_0^2 \right)^2 (\nabla A_{\mu z}) \cdot (\nabla A_{\lambda z}^*) A_{\mu z}^* A_{\lambda z} \left. \right]. \tag{B1}
\end{aligned}$$

As can be seen in Fig. 11, however, $C_0(\varepsilon) - 1$ remains almost zero irrespective of the δ_n -value except at low enough values of $2\pi T\tau$, and it is quantitatively negligible in the temperature region where $2\pi T\tau \gg 1$ is satisfied. Therefore, we can proceed with our analysis without incorporating the impurity-induced vertex correction to the pairing process in the FL gradient term even in the limit of strong anisotropy.

In another gradient terms stemming from the ‘‘Gor’kov box,’’ i.e., the ordinary weak-coupling $O(|\Delta|^4)$ term unac-

energy arising from the Fermi liquid repulsive interaction will be discussed. In our previous work [6], such a vertex correction was not taken into account there by assuming a weak anisotropy.

Since, in the present work, only a straight vortex line extending along \hat{z} is considered, the z -derivative does not have to be included in the gradient terms. Then, the only vertex correction in the FL-corrected gradient terms is the factor $C_0 - 1$ accompanying $A_{\rho z}$ in Eq. (28). For instance, the terms including $A_{\mu z}$ in the first line of Eq. (28) have to be replaced by

companied by a repulsive interaction between quasiparticles, the vertex corrections other than $C_0 - 1$ are also present. As shown in Sec. V of Ref. [6], this weak-coupling diagram does not contribute to the stability of HQVs in the polar and A phases irrespective of how the gradients operate onto the order parameter fields. Furthermore, as explained in relation to Fig. 7, the weak coupling $O(|\Delta|^4)$ term plays only negligible roles for the stability of a HQV-pair occurring in the B phase.

-
- [1] S. Autti, V. V. Dmitriev, J. T. Makinen, A. A. Soldatov, G. E. Volovik, A. N. Yudin, V. V. Zavjalov, and V. B. Eltsov, *Phys. Rev. Lett.* **117**, 255301 (2016).
- [2] K. Aoyama and R. Ikeda, *Phys. Rev. B* **73**, 060504(R) (2006).
- [3] V. V. Dmitriev, A. A. Senin, A. A. Soldatov, and A. N. Yudin, *Phys. Rev. Lett.* **115**, 165304 (2015).
- [4] G. E. Volovik and V. P. Mineev, *JETP Lett.* **24**, 561 (1976).
- [5] M. M. Salomaa and G. E. Volovik, *Phys. Rev. Lett.* **55**, 1184 (1985).
- [6] N. Nagamura and R. Ikeda, *Phys. Rev. B* **98**, 094524 (2018).
- [7] J. T. Makinen, V. V. Dmitriev, J. Nissinen, J. Rysti, G. E. Volovik, A. N. Yudin, K. Zhang, and V. B. Eltsov, *Nat. Commun.* **10**, 237 (2019).
- [8] G. E. Volovik, *JETP Lett.* **52**, 358 (1990).
- [9] M. A. Silaev, E. V. Thuneberg, and M. Fogelstrom, *Phys. Rev. Lett.* **115**, 235301 (2015).
- [10] T. W. B. Kibble, G. Lazarides, and Q. Shafi, *Phys. Rev. D* **26**, 435 (1982).
- [11] E. V. Thuneberg, *Phys. Rev. B* **36**, 3583 (1987).
- [12] M. M. Salomaa and G. E. Volovik, *Rev. Mod. Phys.* **59**, 533 (1987).
- [13] V. V. Dmitriev, A. A. Soldatov, and A. N. Yudin, *Phys. Rev. Lett.* **120**, 075301 (2018).
- [14] G. E. Volovik, *JETP Lett.* **109**, 499 (2019).
- [15] I. A. Fomin, *JETP* **127**, 933 (2018).
- [16] N. Nagamura and R. Ikeda, [arXiv:1905.02569](https://arxiv.org/abs/1905.02569).
- [17] P. W. Anderson, *J. Phys. Chem. Solids* **11**, 26 (1959).
- [18] V. B. Eltsov, T. Kamppinen, J. Rysti, and G. E. Volovik, [arXiv:1908.01645](https://arxiv.org/abs/1908.01645).
- [19] T. Hisamitsu, M. Tange, and R. Ikeda, *Phys. Rev. B* **101**, 100502(R) (2020).
- [20] N. R. Werthamer, in *Superconductivity*, edited by R. D. Parks (Taylor and Francis, London, 1968), Vol. 1.
- [21] S. Yang and R. Ikeda, *J. Phys. Soc. Jpn.* **83**, 084602 (2014).
- [22] T. Ohmi, T. Tsuneto, and T. Fujita, *Prog. Theor. Phys.* **70**, 647 (1983).
- [23] D. Volhardt and P. Wolfe, *The Superfluid Phases of Helium 3* (Taylor and Francis, London, 2002).
- [24] E. V. Thuneberg, S. K. Yip, M. Fogelstrom, and J. A. Sauls, *Phys. Rev. Lett.* **80**, 2861 (1998).
- [25] J. Rystia, A. N. Yudin, J. T. Makinen, V. V. Dmitriev, and V. B. Eltsov (unpublished).
- [26] V. V. Dmitriev, M. S. Kutuzov, A. A. Soldatov, and A. N. Yudin, *JETP Lett.* **110**, 734 (2019).
- [27] D. A. Ivanov, *Phys. Rev. Lett.* **86**, 268 (2001); G. E. Volovik, *JETP Lett.* **70**, 609 (1999).